A numerical method for ocean-acoustic normal modes[a)]

Michael Porter and Edward L. Reiss
Department of Engineering Sciences and Applied Mathematics, Northwestern University, Evanston, Illinois 60201

(Received 19 August 1983; accepted for publication 25 January 1984)

The method of normal modes is frequently used to solve acoustic propagation problems in stratified oceans. The propagation numbers for the modes are the eigenvalues of the boundary value problem to determine the depth dependent normal modes. Errors in the numerical determination of these eigenvalues appear as phase shifts in the range dependence of the acoustic field. Such errors can severely degrade the accuracy of the normal mode representation, particularly at long ranges. In this paper we present a fast finite difference method to accurately determine these propagation numbers and the corresponding normal modes. It consists of a combination of well-known numerical procedures such as Sturm sequences, the bisection method, Newton's and Brent's methods, Richardson extrapolation, and inverse iteration. We also introduce a modified Richardson extrapolation procedure that substantially increases the speed and accuracy of the computation.

PACS numbers: 43.30.Bp, 43.20.Bi, 92.10.Vz, 43.30.Jx

INTRODUCTION

The acoustic pressure produced by a time harmonic point source in a stratified ocean of constant depth D has a normal mode representation, which is proportional to

$$p(r,z,t) = e^{-i\omega t} \sum_{j=1}^{\infty} \phi_j(z_0)\phi_j(z) H_0^{(1)}(\lambda_j r). \tag{1}$$

Here, the dimensionless radial and depth variables r and z are obtained by dividing the dimensional variables by D (the z coordinate is directed downward from the ocean's surface), $H_0^{(1)}(r)$ is the Hankel function of order zero and of the first kind and ω and z_0 are the angular frequency and depth of the source, respectively. In addition, the propagation numbers λ_j and the normal modes $\phi_j(z)$ are the eigenvalues and eigenfunctions, respectively, of

$$\phi'' + [k^2/c^2(z) - \lambda^2]\phi = 0, \quad \text{for } 0 < z < 1, \tag{2}$$

$$\phi(0) = 0, \quad \phi'(1) = 0. \tag{3}$$

In (2), $c(z)$ is a dimensionless ocean sound speed that is obtained by scaling the physical sound speed by a reference sound speed c_0, and k^2 is the dimensionless wavenumber that is defined by

$$k^2 \equiv \omega^2 D^2 / c_0^2. \tag{4}$$

The boundary conditions in (3) imply that the ocean surface $z = 0$ is free, i.e., it is the pressure release condition, and the ocean bottom $z = 1$ is rigid.

In (1), the eigenfunctions are normalized by the conditions

$$\int_0^1 \phi_j^2(z)dz = 1, \quad j = 1,2,\ldots . \tag{5}$$

There are only a finite number of eigenvalues λ_j of (2) that are real. Then by the properties of the Hankel function they correspond to propagating modes in the sum (2). The remaining eigenvalues correspond to evanescent or nonpropagating modes. By employing the large argument asymptotic expansion of the Hankel function we obtain the farfield representation as

$$p = \frac{e^{-i\pi/4}}{4}\left(\frac{2}{\pi r}\right)^{1/2} \sum_{j=1}^{\infty} \phi_j(z_0)\phi_j(z)\lambda_j^{-1/2} e^{i(\lambda_j r - \omega t)}. \tag{6}$$

Explicit solutions of (2) can be obtained only for relatively simple sound speed profiles $c(z)$. The profiles encountered in the ocean are usually sufficiently complex that numerical methods are employed to solve (2). For example, coefficient approximation methods[1,2] and shooting methods[3,4] are widely used. Typically, the errors in the eigenvalues λ_j that are determined from numerical solutions of (2) increase with j. Furthermore, as we observe from either (1) or (6) these errors appear as phase shifts in the range dependence of p. Specifically, the phase shifts are porportional to the products of these errors and r. Thus, if r is large, as occurs in long-range propagation, the phase shifts caused by the numerical errors in λ_j will seriously degrade the accuracy of the series representations (1) and (6). This suggests the need for extremely accurate determination of the eigenvalues of (2).

In addition, we observe that if k is large, which occurs for "high-" frequency sources and/or deep oceans, the number of propagating modes is large. These and other factors in the repeated use of (1) to represent acoustic fields suggest that the numerical methods must be fast in addition to accurate. In this paper we present a numerical procedure which satisfies these requirements. It is a combination of known numerical techniques such as finite difference approximations and Richardson extrapolation.

The method is described in Sec. II and it is then applied in Sec. III to two examples to demonstrate its speed and accuracy. The Munk profile[5] is employed for the sound speed in the first example. The second example demonstrates the ability of the method to handle sound speed profiles with multiple ducts. This particular double-duct profile

[a)] The research reported in this paper was supported by the National Science Foundation under Grant No. MCS 8300578, and the Office of Naval Research under Contract No. N00014-83-C-0518.

 0001-4966/84/070244-09$00.80

is difficult to solve numerically because of the approximate symmetry of the ducts and the concomitant near-degeneracy of the eigenvalues.

In Sec. IV we present a brief discussion of the relationship between the present method and shooting methods for solving (2). A possible improvement in these shooting methods is suggested by this discussion. Applications and extensions of the method to more complicated ocean acoustics problems such as propagation from a time harmonic source in an ocean resting on an elastic bottom will be presented in future publications. Then modifications in the numerical methods are required for treating the elastic bottom, as we will demonstrate.

I. THE METHOD

To solve (2) numerically we first define a mesh by dividing the interval $0<z<1$ into N equal intervals by the points $z_i = ih$, $i = 0,1,...,N$ where the mesh width h is defined by $h = 1/N$. Then using the standard three point difference approximation to the second derivative in (2) and the centered difference approximation to the first derivative in (3), we obtain the algebraic eigenvalue problem

$$A\phi = \mu\phi; \quad \mu \equiv \lambda^2 h^2 \tag{7}$$

as an approximation to the eigenvalue problem (2). Here, ϕ is the N-dimensional vector with components ϕ_1, ϕ_2,..., ϕ_N. These components are approximations to the eigenfunctions of (2) evaluated at the mesh points. In addition, the tridiagonal $N \times N$ matrix A is defined by

$$A \equiv \begin{bmatrix} a_1 & 1 & 0 & 0 & \cdots & \cdots & 0 \\ 1 & a_2 & 1 & 0 & \cdots & \cdots & 0 \\ 0 & 1 & a_3 & 1 & 0 & \cdots & 0 \\ & & \ddots & \ddots & \ddots & & \\ 0 & \cdots & \cdots & 0 & 1 & a_{N-1} & 1 \\ 0 & \cdots & \cdots & \cdots & 0 & 2 & a_N \end{bmatrix}, \tag{8}$$

where the coefficients a_i are defined by

$$a_i = 2 - k^2 h^2 / c^2(z_i), \quad i = 1,2,...,N. \tag{9}$$

We use the Sturm sequence method[6,7] to solve the algebraic eigenvalue problem (7) for a fixed mesh size N. Thus we consider the sequence $S_1, S_2,...,S_N$ which is defined by

$$\begin{aligned} &S_0 \equiv 1, \quad S_1 \equiv \mu - a_1, \\ &S_i \equiv (\mu - a_i)S_{i-1} - S_{i-2}, \quad i = 2,...,N-1, \\ &S_N \equiv (\mu - a_N)S_{N-1} - 2S_{N-2}. \end{aligned} \tag{10}$$

This sequence has the following two properties that we employ:

(1) S_i is the ith principal minor of the matrix $\mu I - A$, so that S_N is the characteristic polynomial.

(2) For a fixed μ, the number of sign changes in the sequence $\{S_i\}$ is equal to the number of eigenvalues greater than μ, where zeros in the sequence are deleted.

In the first step of the method we find an isolating interval for each eigenvalue μ_j, i.e., an interval in μ which contains only the eigenvalue μ_j. For the first, or largest, eigenvalue an upper bound is obtained from Gerschgorin's theorem.[6] Zero is taken as the lower bound since only propagating modes (positive eigenvalues) are to be obtained. This interval is successively bisected until it contains only the first eigenvalue, a condition that is determined by counting the sign changes in the Sturm sequence. This process is repeated for each subsequent eigenvalue. Now, however, the previous eigenvalue's lower bound is an upper bound for the next eigenvalue. In addition, lower bounds for the current eigenvalue may have already been computed during the bisection process for the previous eigenvalues. The isolating intervals provide initial estimates for each eigenvalue. More accurate approximations of each eigenvalue are then obtained by solving the characteristic equation by Brent's method[8] which combines bisection, linear interpolation, and inverse quadratic interpolation. Convergence is then guaranteed to the isolated eigenvalue.

In Richardson's extrapolation method[9,10] improved estimates of the eigenvalues of the continuous problem (2) are obtained from the approximations of the eigenvalues $\mu_j(h)$ of the algebraic problem (7). In the standard extrapolation method the converged numerical value with mesh width h for the jth eigenvalue $\mu_j(h)$ is expressed as

$$\mu_j(h) = \mu_j^0 + b_2 h^2 + b_4 h^4 + \cdots + b_{2(m-1)} h^{2(m-1)}. \tag{11}$$

Here, μ_j^0/h^2 is the Richardson approximation to λ_j^2, the square of the jth eigenvalue of (2). The constant μ_j^0 is then determined from the algebraic system that results from applying (11) to a sequence of successively finer meshes $\{h_j\} = h_1, h_2,...,h_m$. Since this approximation depends on the sequence of mesh widths that is employed we denote the Richardson approximation corresponding to the meshes h_p, h_{p+1},..., h_{p+q} by $\mu_j^0(p,...,p+q)$. Successive extrapolations are generated recursively by the relation

$$\mu_j^0(p,...,p+q) = \frac{h_p^2 \mu_j^0(p+1,...,p+q) - h_{p+q}^2 \mu_j^0(p,...,p+q-1)}{h_p^2 - h_{p+q}^2} \tag{12}$$

as we can obtain from (11).

In this paper we employ a modified Richardson extrapolation procedure which was motivated by the analysis in Ref. 11. Thus the Richardson expansion (11) is now replaced by

$$\mu_j^0(h) - [\mu_j^I(h) - \mu_j^I(0)] = \hat{\mu}_j^0 + b_2 h^2 + b_4 h^4 + \cdots + b_{2(m-1)} h^{2(m-1)}. \tag{13}$$

Here the eigenvalues $\mu_j^I(0)$ and $\mu_j^I(h)$, which are defined by

$$\begin{aligned} &\mu_j^I(0) \equiv h^2[k^2 - (j - \tfrac{1}{2})^2 \pi^2], \\ &\mu_j^I(h) \equiv h^2(k^2 - \{[\sin(j - \tfrac{1}{2})\pi h/2]/(h/2)\}^2), \end{aligned} \tag{14}$$

are the exact eigenvalues of (2) and (7), respectively, with $c \equiv 1$. That is, they are the exact eigenvalues of the continuous and algebraic eigenvalue problems for the isovelocity profile. Then the modified Richardson approximations $\hat{\mu}_j^0$ are computed as before but now using (13). The recursion formula (12) also applies to these modified extrapolation eigenvalues. The analysis in Ref. 11 suggests that the modified extrapolation method moderates the error growth with increasing mode number.

The Sturm sequence procedure for isolating each eigenvalue of the algebraic system is used only for the first mesh,

i.e., for $h = h_1$, and not for the subsequent meshes. Initial guesses for the eigenvalues corresponding to the second and subsequent meshes are obtained by using the modified extrapolation procedure but extrapolating to the desired mesh size. Thus, for the second and subsequent meshes, isolating intervals for the eigenvalues are not obtained and Brent's method is not applicable. Therefore, Newton's method is employed, starting from the initial guesses to solve for the numerical eigenvalues.

The mesh selection is motivated by two considerations. First, if the mesh is refined too rapidly, then the initial guess obtained from the previous mesh may be sufficiently inaccurate that the Newton iteration converges to the wrong mode. Furthermore, if the meshes are refined too slowly then the extrapolation is not as effective. We have found it convenient to use the following meshes:

$$N = \left[\frac{3m}{100}(100,120,150,190,250,320,400,500)\right], \tag{15a}$$

$$m \equiv [k/\pi]. \tag{15b}$$

Here, m is an estimate of the number of propagating modes which is obtained from the isovelocity profile, $c \equiv 1$. The square brackets in (15) denote the integer part of the quantity.

After the eigenvalues are obtained to the desired accuracy, the eigenvectors are found by inverse iteration[6,7] using the difference equations and eigenvalues of the final mesh.

A related extrapolation method was previously developed for the one-dimensional Schrödinger equation.[12] The present method has the following new features which provide improved speed and accuracy.

(1) A quadratically convergent root finder is employed rather than the linearly convergent method of bisection presumably used in Ref. 12.

(2) The eigenvalues of the previous mesh are used to provide the initial guesses for the eigenvalues of the next refined mesh.

(3) We use a modified Richardson extrapolation procedure.

Finally, we remark that we have experimented with generalizations of our finite difference methods by using Numerov's method[3] and a five-point difference scheme to obtain more accurate approximations to (2). We find that the standard three-point difference scheme is both simpler to implement and more efficient than these higher order schemes. When a fourth-order difference scheme, such as Numerov's method, is used in the extrapolation procedure, the error in the eigenvalues has the following form:

$$\mu_j(h) = \mu_j^0 + b_4 h^4 + b_6 h^6 + \cdots . \tag{16}$$

Consequently, each extrapolation increases the order of the method by two, and after L extrapolations it is a $4 + 2(L-1)$ order method. This same order can be obtained with $L+1$ extrapolations using the standard three-point difference scheme; however, the standard scheme requires about half as much computation time for the same number of mesh points.

We have also applied extrapolation techniques to a coefficient approximation scheme using constant sound speed layers and find the present method to be more efficient.

II. APPLICATIONS OF THE METHOD

We now present two applications of our method to demonstrate its convergence properties, speed, accuracy, and versatility. In the first problem we consider a deep ocean with a Munk sound speed profile. Thus we have

TABLE I. Numerical eigenvalues $\xi_j(p) = [\mu_j(p)/h^2] \times 10^3/(5000)^2$ for the Munk profile.

$N=$	268	321	402	509
ET =	2.8570	1.5820	1.6980	1.5970
j	$\xi_j(1)$	$\xi_j(2)$	$\xi_j(3)$	$\xi_j(4)$
1	3.356 383 1	3.356 382 7	3.356 382 4	3.356 382 2
5	3.299 100 5	3.299 087 5	3.299 076 6	3.299 069 4
9	3.247 071 8	3.247 031 9	3.246 998 7	3.246 976 8
13	3.198 774 6	3.198 697 6	3.198 633 4	3.198 591 0
17	3.154 173 1	3.154 063 0	3.153 971 3	3.153 910 8
21	3.104 375 0	3.104 117 2	3.103 902 1	3.103 759 7
25	3.036 810 4	3.036 299 1	3.035 872 5	3.035 589 9
29	2.955 900 9	2.954 981 9	2.954 214 4	2.953 705 8
33	2.862 521 6	2.860 984 3	2.859 699 6	2.858 847 7
37	2.757 124 2	2.754 695 9	2.752 665 1	2.751 317 6
41	2.640 058 2	2.636 397 0	2.633 332 5	2.631 297 9
45	2.511 644 9	2.506 332 5	2.501 881 9	2.498 924 9
49	2.372 204 3	2.364 739 3	2.358 478 9	2.354 316 5
53	2.222 066 5	2.211 857 5	2.203 286 9	2.197 583 8
57	2.061 576 8	2.047 936 7	2.036 472 6	2.028 837 5
61	1.891 098 4	1.873 238 2	1.858 209 1	1.848 190 5
65	1.711 013 3	1.688 037 1	1.668 677 7	1.655 759 9
69	1.521 722 5	1.492 622 0	1.468 068 7	1.451 668 1
73	1.323 645 9	1.287 296 4	1.256 581 8	1.236 043 1
77	1.117 221 8	1.072 377 5	1.034 426 3	1.009 019 1
81	0.902 906 22	0.848 196 84	0.801 821 45	0.770 736 41
85	0.681 117 85	0.615 099 53	0.558 996 05	0.521 341 91
89	0.452 507 47	0.373 444 05	0.306 188 65	0.260 988 84

TABLE II. Errors in numerical eigenvalues $e_j(p) = [\lambda_j - \mu(p)/h^2]/(5000)^2$ for the Munk profile.

$N=$	268	321	402	509
ET =	2.8570	1.5820	1.6980	1.5970
j	$e_j(1)$	$e_j(2)$	$e_j(3)$	$e_j(4)$
1	−1.2E−09	−8.7E−10	−5.6E−10	−3.4E−10
5	−4.3E−08	−3.0E−08	−1.9E−08	−1.1E−08
9	−1.3E−07	−9.1E−08	−5.8E−08	−3.6E−08
13	−2.5E−07	−1.7E−07	−1.1E−07	−7.0E−08
17	−3.6E−07	−2.5E−07	−1.6E−07	−1.0E−07
21	−8.5E−07	−5.9E−07	−3.7E−07	−2.3E−07
25	−1.6E−06	−1.1E−06	−7.5E−07	−4.6E−07
29	−3.0E−06	−2.1E−06	−1.3E−06	−8.4E−07
33	−5.0E−06	−3.5E−06	−2.2E−06	−1.4E−06
37	−8.0E−06	−5.6E−06	−3.5E−06	−2.2E−06
41	−1.2E−05	−8.4E−06	−5.4E−06	−3.3E−06
45	−1.7E−05	−1.2E−05	−7.8E−06	−4.9E−06
49	−2.4E−05	−1.7E−05	−1.1E−05	−6.9E−06
53	−3.3E−05	−2.3E−05	−1.5E−05	−9.5E−06
57	−4.5E−05	−3.1E−05	−2.0E−05	−1.2E−05
61	−5.9E−05	−4.1E−05	−2.6E−05	−1.6E−05
65	−7.6E−05	−5.3E−05	−3.4E−05	−2.1E−05
69	−9.7E−05	−6.8E−05	−4.3E−05	−2.7E−05
73	−1.2E−04	−8.5E−05	−5.4E−05	−3.4E−05
77	−1.5E−04	−1.0E−04	−6.8E−05	−4.2E−05
81	−1.8E−04	−1.2E−04	−8.3E−05	−5.2E−05
85	−2.2E−04	−1.5E−04	−1.0E−04	−6.3E−05
89	−2.6E−04	−1.8E−04	−1.2E−04	−7.6E−05

$$k = 290, \quad c(z) = 1 + 0.00737(x - 1 + e^x),$$
$$\text{where } x(z) \equiv 100z/13 - 1, \tag{17}$$

where we have used parameter values suggested by Dozier[3]; see Ref. 5 for a typical graph of $c(z)$. In Table I we present selected scaled numerically determined eigenvalues ξ_j of the corresponding algebraic problems (7) for the mesh widths indicated in the table. Recall that $h = 1/N$, and see Table I for the definition of ξ_j. In Table II the errors $e(j)$ in these numerical eigenvalues are shown. The error is the difference between the numerically determined eigenvalues given in Table I and the "exact" eigenvalues. The exact eigenvalues are defined as numerically determined by our method using extrapolations with several more refined meshes. We observe that for each mesh the errors increase monotonically with the mode number j. The symbol ET in the tables denotes the execution time in seconds on the Northwestern Cyber 170/730 to compute all the eigenvalues correspond-

TABLE III. Standard extrapolations $\xi_j(p,\ldots,p+q) = [u_j^0(p,\ldots,p+q)/h^2] \times 10^3/(5000)^2$ for the Munk profile.

$N=$	268	321	402	509
j	$\xi_j(1)$	$\xi_j(1,2)$	$\xi_j(1,2,3)$	$\xi_j(1,2,3,4)$
1	3.356 383 146 9	3.356 381 886 2	3.356 381 886 3	3.356 381 886 3
5	3.299 100 567 8	3.299 057 468 1	3.299 057 492 9	3.299 057 492 8
9	3.247 071 815 6	3.246 940 310 5	3.246 940 454 3	3.246 940 454 1
13	3.198 774 631 5	3.198 520 408 0	3.198 520 805 0	3.198 520 804 1
17	3.154 173 141 7	3.153 809 665 1	3.153 810 587 8	3.153 810 581 4
21	3.104 375 068 2	3.103 523 956 4	3.103 523 706 2	3.103 523 702 4
25	3.036 810 401 6	3.035 122 929 6	3.035 121 178 2	3.035 121 167 9
29	2.955 900 926 9	2.952 867 423 6	2.952 861 627 8	2.952 861 605 1
33	2.862 521 636 2	2.857 447 218 3	2.857 432 837 6	2.857 432 790 7
37	2.757 124 228 5	2.749 108 991 6	2.749 078 358 9	2.749 078 264 8
41	2.640 058 204 5	2.627 973 488 7	2.627 914 430 2	2.627 914 247 6
45	2.511 644 935 7	2.494 109 953 3	2.494 004 068 3	2.494 003 724 7
49	2.372 204 389 0	2.347 563 700 9	2.347 384 262 2	2.347 383 635 4
53	2.222 066 584 4	2.188 368 587 0	2.188 078 029 2	2.188 076 920 4
57	2.061 576 888 3	2.016 553 417 0	2.016 100 382 0	2.016 098 478 5
61	1.891 098 469 1	1.832 145 608 0	1.831 461 519 6	1.831 458 343 7
65	1.711 013 319 9	1.635 173 499 4	1.634 168 640 2	1.634 163 481 5
69	1.521 722 500 3	1.425 667 959 1	1.424 227 027 4	1.424 218 853 7
73	1.323 645 921 9	1.203 663 606 3	1.201 640 730 5	1.201 628 074 8
77	1.117 221 851 8	0.969 199 819 37	0.966 413 013 06	0.966 393 829 85
81	0.902 906 229 44	0.722 321 620 31	0.718 546 661 74	0.718 518 148 31
85	0.681 171 853 07	0.463 080 487 83	0.458 044 212 18	0.458 002 588 93
89	0.452 507 470 56	0.191 535 128 86	0.184 908 123 41	0.184 848 366 49

TABLE IV. Errors in standard extrapolations $e_j(p,\ldots,p+q) = [\lambda_j - \mu_j^0(p,\ldots,p+q)/h^2]/(5000)^2$ for the Munk profile.

$N=$	268	321	402	509
j	$e_j(1)$	$e_j(1,2)$	$e_j(1,2,3)$	$e_j(1,2,3,4)$
1	−1.2E−09	1.4E−13	...	...
5	−4.3E−08	2.4E−11	−2.0E−14	...
9	−1.3E−07	1.4E−10	−2.0E−13	...
13	−2.5E−07	3.9E−10	−8.3E−13	...
17	−3.6E−07	9.1E−10	−6.3E−12	...
21	−8.5E−07	−2.5E−10	−3.7E−12	...
25	−1.6E−06	−1.7E−09	−1.0E−11	2.6E−14
29	−3.0E−06	−5.8E−09	−2.2E−11	6.5E−14
33	−5.0E−06	−1.4E−08	−4.6E−11	1.4E−13
37	−8.0E−06	−3.0E−08	−9.3E−11	2.8E−13
41	−1.2E−05	−5.9E−08	−1.8E−10	5.1E−13
45	−1.7E−05	−1.0E−07	−3.4E−10	8.6E−13
49	−2.4E−05	−1.8E−07	−6.2E−10	1.3E−12
53	−3.3E−05	−2.9E−07	−1.1E−09	1.9E−12
57	−4.5E−05	−4.5E−07	−1.9E−09	2.6E−12
61	−5.9E−05	−6.8E−07	−3.1E−09	3.1E−12
65	−7.6E−05	−1.0E−06	−5.1E−09	3.0E−12
69	−9.7E−05	−1.4E−06	−8.1E−09	1.6E−12
73	−1.2E−04	−2.0E−06	−1.2E−08	−2.3E−12
77	−1.5E−04	−2.8E−06	−1.9E−08	−1.0E−11
81	−1.8E−04	−3.8E−06	−2.8E−08	−2.7E−11
85	−2.2E−04	−5.0E−06	−4.1E−08	−5.5E−11
89	−2.6E−04	−6.6E−06	−5.9E−08	−1.0E−10

ing to each mesh width.

The results of successive standard Richardson extrapolations are shown in Tables III and IV. Of course, the first columns in Tables II and IV are equal. However, a comparison of the subsequent columns in Tables II and IV shows the dramatic decrease in the errors that are achieved by the extrapolation. Typically, each successive extrapolation reduces the error by a factor of 100–1000. The 100-fold error reduction which is obtained with one additional extrapolation would require a ten times finer mesh and a similar increase in execution time if it were obtained simply by mesh reduction. The dots in the tables indicate errors which are within the accuracy of the root finding technique. They are not explicitly given because they are believed to be insignificantly small.

The eigenvalues obtained using the modified extrapolation process are given in Tables V and VI. In comparison to the standard extrapolations of Tables III and IV, the growth

TABLE V. Modified extrapolations $\hat{\xi}_j(p,\ldots,p+q) = [\hat{\mu}_j^0(p,\ldots,p+q)/h^2] \times 10^3/(5000)^2$ for the Munk profile.

$N=$	268	321	402	509
j	$\hat{\xi}_j(1)$	$\hat{\xi}_j(1,2)$	$\hat{\xi}_j(1,2,3)$	$\hat{\xi}_j(1,2,3,4)$
1	3.356 383 146 6	3.356 381 886 2	3.356 381 886 3	3.356 381 886 3
5	3.299 098 714 2	3.299 057 468 0	3.299 057 492 9	3.299 057 492 8
9	3.247 048 224 9	3.246 940 305 1	3.246 940 454 3	3.246 940 454 1
13	3.198 664 341 0	3.198 520 353 0	3.198 520 805 0	3.198 520 804 1
17	3.153 838 482 4	3.153 809 374 2	3.153 810 587 7	3.153 810 581 4
21	3.103 578 197 0	3.103 522 887 0	3.103 523 705 7	3.103 523 702 4
25	3.035 186 053 8	3.035 119 815 9	3.035 121 176 2	3.035 121 167 9
29	2.952 929 448 9	2.952 859 714 9	2.952 861 620 9	2.952 861 605 1
33	2.857 502 357 7	2.857 430 284 0	2.875 432 818 1	2.857 432 790 6
37	2.749 149 232 3	2.749 075 050 6	2.749 078 309 5	2.749 078 264 8
41	2.627 986 552 0	2.627 910 227 1	2.627 914 316 8	2.627 914 247 5
45	2.494 077 404 7	2.493 998 791 6	2.494 003 827 8	2.494 003 724 5
49	2.347 458 779 2	2.347 377 675 5	2.347 383 784 0	2.347 383 634 9
53	2.188 153 644 8	2.188 069 810 4	2.188 077 128 9	2.188 076 919 3
57	2.016 176 920 1	2.016 090 084 9	2.016 098 764 4	2.016 098 476 3
61	1.831 538 654 3	1.831 448 521 2	1.831 458 727 8	1.831 458 339 4
65	1.634 245 826 6	1.634 152 071 2	1.634 163 988 6	1.634 163 473 2
69	1.424 303 412 0	1.424 205 681 4	1.424 219 513 0	1.424 218 838 7
73	1.201 715 038 0	1.201 612 948 1	1.201 628 919 9	1.201 628 048 5
77	0.966 483 402 70	0.966 376 535 37	0.966 394 899 14	0.966 393 784 78
81	0.718 610 549 37	0.718 498 448 21	0.718 519 485 14	0.718 518 073 40
85	0.458 098 050 49	0.457 980 216 36	0.458 004 241 35	0.458 002 467 47
89	0.184 947 134 63	0.184 823 020 29	0.184 850 386 78	0.184 848 173 95

TABLE VI. Errors in modified extrapolations $\hat{e}_j(p,\ldots,p+q) = [\lambda_j - \hat{\mu}_j^0(p,\ldots,p+q)/h^2]/(5000)^2$ for the Munk profile.

$N=$	268	321	402	509
j	$\hat{e}_j(1)$	$\hat{e}_j(1,2)$	$\hat{e}_j(1,2,3)$	$\hat{e}_j(1,2,3,4)$
1	$-1.2E-09$	$1.4E-13$	...	...
5	$-4.1E-08$	$2.4E-11$	$-2.0E-14$	...
9	$-1.0E-07$	$1.4E-10$	$-2.0E-13$	...
13	$-1.4E-07$	$4.5E-10$	$-8.2E-13$	...
17	$-2.7E-08$	$1.2E-09$	$-6.2E-12$	...
21	$-5.4E-08$	$8.1E-10$	$-3.2E-12$	...
25	$-6.4E-08$	$1.3E-09$	$-8.3E-12$	$2.7E-14$
29	$-6.7E-08$	$1.8E-09$	$-1.5E-11$	$6.7E-14$
33	$-6.9E-08$	$2.5E-09$	$-2.7E-11$	$1.5E-13$
37	$-7.0E-08$	$3.2E-09$	$-4.4E-11$	$3.1E-13$
41	$-7.2E-08$	$4.0E-09$	$-6.8E-11$	$5.9E-13$
45	$-7.3E-08$	$4.9E-09$	$-1.0E-10$	$1.0E-12$
49	$-7.5E-08$	$5.9E-09$	$-1.4E-10$	$1.8E-12$
53	$-7.6E-08$	$7.1E-09$	$-2.0E-10$	$3.0E-12$
57	$-7.8E-08$	$8.3E-09$	$-2.8E-10$	$4.8E-12$
61	$-8.0E-08$	$9.8E-09$	$-3.8E-10$	$7.4E-12$
65	$-8.2E-08$	$1.1E-08$	$-5.0E-10$	$1.1E-11$
69	$-8.4E-08$	$1.3E-08$	$-6.5E-10$	$1.6E-11$
73	$-8.6E-08$	$1.5E-08$	$-8.4E-10$	$2.4E-11$
77	$-8.9E-08$	$1.7E-08$	$-1.0E-09$	$3.4E-11$
81	$-9.2E-08$	$1.9E-08$	$-1.3E-09$	$4.7E-11$
85	$-9.5E-08$	$2.2E-08$	$-1.7E-09$	$6.6E-11$
89	$-9.8E-08$	$2.5E-08$	$-2.1E-09$	$9.0E-11$

in the error with increasing mode number is dramatically reduced. This occurs particularly for the coarser meshes. Thus the numerical results suggest that if the speed of computation is a controlling factor in the computation, so that the least refined mesh consistent with accuracy is desired, the modified extrapolation procedure then becomes more effective.

Some selected numerically determined modes are shown in Fig. 1. For convenience in presenting the graphs,

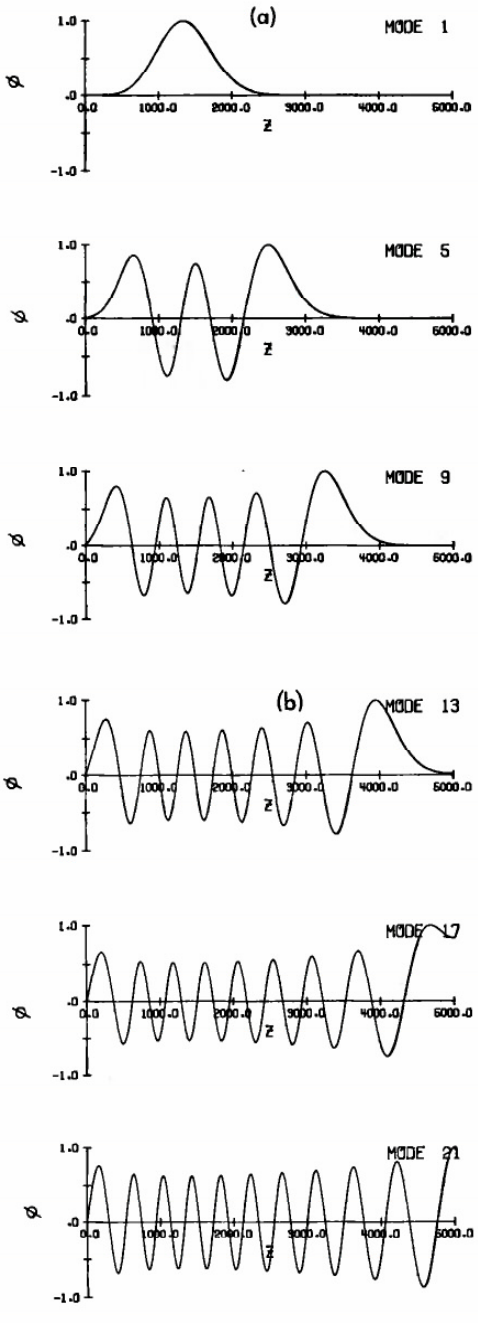

FIG. 1. Selected modes for Munk sound speed profile as a function of Z.

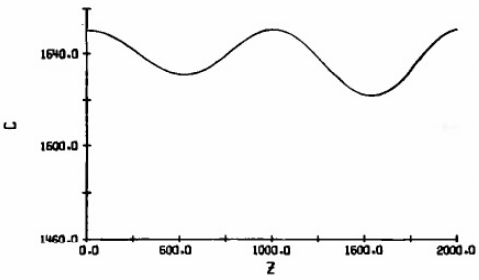

FIG. 2. Sound speed profile for the double-duct problem for an ocean of depth $D = 2000$ m as a function of the dimensional depth variable Z.

the modes have been normalized by

$$\max_{0<z<1} |\phi(z)| = 1,$$

rather than by (5). With these parameter values only modes 17 and 18 are refracted-surface reflected modes.

We now consider the double-duct profile sketched in Fig. 2, where

$$k^2 = 64\,000, \quad c^2 = \frac{1}{1 + (0.6 + 0.8z)(1 - \cos 4\pi z)/64}. \tag{18}$$

The first nine eigenvalues at several meshes are displayed in Tables VII and VIII and the corresponding eigenfunctions

TABLE VII. Numerical eigenvalues $\xi_j(p) = [\mu_j(p)/h^2] \times 10^3/(2000)^2$ for the double-duct problem.

$N =$	120	144	180	228
ET =	0.1670	0.0980	0.0910	0.1000
j	$\xi_j(1)$	$\xi_j(2)$	$\xi_j(3)$	$\xi_j(4)$
1	1.652 698	1.652 695	1.652 693	1.652 691
2	1.638 335	1.638 322	1.638 312	1.638 305
3	1.634 161	1.634 159	1.634 158	1.634 157
4	1.625 217	1.625 189	1.625 165	1.625 150
5	1.622 580	1.622 572	1.622 566	1.622 561
6	1.613 684	1.613 640	1.613 605	1.613 581
7	1.612 290	1.612 272	1.612 285	1.612 249
8	1.604 679	1.604 638	1.604 605	1.604 582
9	1.603 265	1.603 233	1.603 206	1.603 189

TABLE VIII. Errors in numerical eigenvalues $e_j(p) = [\lambda_j - \mu_j(p)/h^2]/(2000)^2$ for the double-duct problem.

$N =$	120	144	180	228
ET =	0.1670	0.0980	0.0910	0.1000
j	$e_j(1)$	$e_j(2)$	$e_j(3)$	$e_j(4)$
1	$-9.2E-08$	$-6.4E-08$	$-4.1E-08$	$-2.5E-08$
2	$-4.1E-07$	$-2.8E-07$	$-1.8E-07$	$-1.1E-07$
3	$-6.0E-08$	$-4.2E-08$	$-2.7E-08$	$-1.6E-08$
4	$-9.3E-07$	$-6.4E-07$	$-4.1E-07$	$-2.5E-07$
5	$-2.6E-07$	$-1.8E-07$	$-1.1E-07$	$-7.2E-08$
6	$-1.4E-06$	$-9.7E-07$	$-6.2E-07$	$-3.8E-07$
7	$-5.6E-07$	$-3.9E-07$	$-2.5E-07$	$-1.5E-07$
8	$-1.3E-06$	$-9.2E-07$	$-5.8E-07$	$-3.6E-07$
9	$-1.0E-06$	$-7.3E-07$	$-4.7E-07$	$-2.9E-07$

are graphed in Fig. 3. For the parameters (18) there are approximately 80 propagating modes. The execution times reflect only the time required to compute the first nine eigenvalues. Successive extrapolations using the modified scheme are given in Tables IX and X.

As may be seen from Tables III–VI the modified extrapolation procedure is superior to the standard Richardson extrapolation with the most dramatic improvements obtained when the error is largest, i.e., for high-order modes, coarse meshes, and low-order extrapolation. For example, the modified extrapolation procedure is particularly effective for the RSRBR (refracted surface-reflected bottom-reflected) modes. In the double-duct problem, in which we computed only the RR (refracted–refracted) modes the standard and modified extrapolation procedures would yield virtually identical results.

The merit of using the modified extrapolation scheme to generate an initial guess is demonstrated in Table XI, in

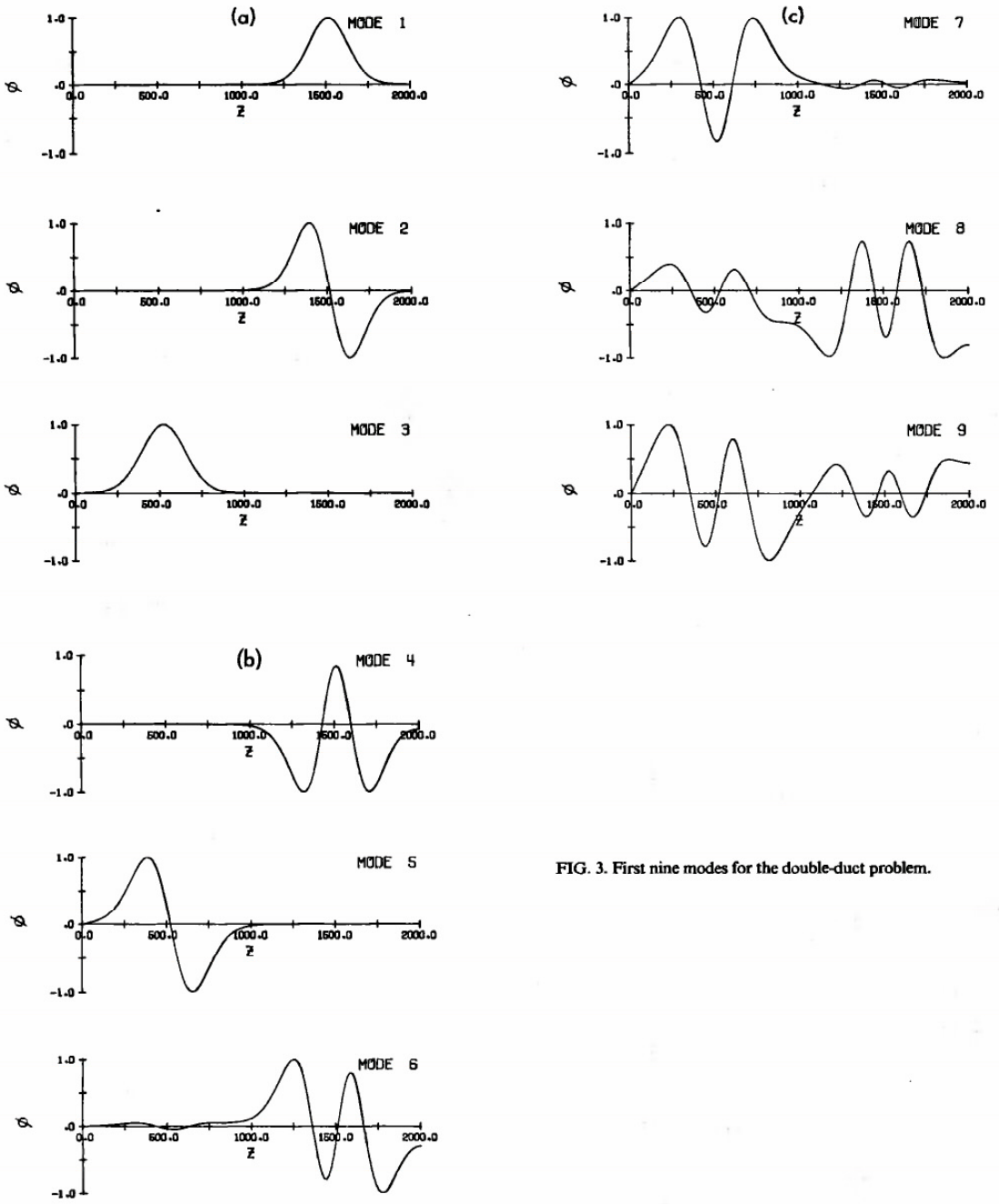

FIG. 3. First nine modes for the double-duct problem.

TABLE IX. Modified extrapolations $\hat{\xi}_j(p,\ldots,p+q) = [\hat{\mu}_j^0(p,\ldots,p+q)/h^2] \times 10^2/(2000)^2$ for the double-duct problem.

$N=$	120	144	180	228
j	$\hat{\xi}_j(1)$	$\hat{\xi}_j(1,2)$	$\hat{\xi}_j(1,2,3)$	$\hat{\xi}_j(1,2,3,4)$
1	1.652 698 326 2	1.652 689 031 8	1.652 689 041 4	1.652 689 041 4
2	1.638 335 370 1	1.638 293 693 7	1.638 293 774 2	1.638 293 774 0
3	1.634 160 876 1	1.634 155 329 9	1.634 155 335 3	1.634 155 335 3
4	1.625 215 526 4	1.625 123 968 3	1.625 124 262 1	1.625 124 261 0
5	1.622 575 057 8	1.622 554 419 7	1.622 554 465 2	1.622 554 465 1
6	1.613 671 164 7	1.613 542 170 9	1.613 542 944 3	1.613 542 941 4
7	1.612 265 095 8	1.612 233 395 2	1.612 233 541 3	1.612 233 540 2
8	1.604 635 314 1	1.604 544 596 4	1.604 546 339 8	1.604 546 329 7
9	1.603 192 349 7	1.603 159 810 5	1.603 159 759 5	1.603 159 758 8

TABLE X. Errors in modified extrapolations $\hat{e}_j(p,\ldots,p+q) = [\lambda_j - \hat{\mu}_j^0(p,\ldots,p+q)/h^2]/(2000)^2$ for the double-duct problem.

$N=$	120	144	180	228
j	$\hat{e}_j(1)$	$\hat{e}_j(1,2)$	$\hat{e}_j(1,2,3)$	$\hat{e}_j(1,2,3,4)$
1	$-9.2E-08$	$9.6E-11$	$-1.6E-13$	...
2	$-4.1E-07$	$8.0E-10$	$-2.3E-12$	$2.9E-14$
3	$-5.5E-08$	$5.3E-11$	$-7.1E-14$	...
4	$-9.1E-07$	$2.9E-09$	$-1.1E-11$	$3.5E-14$
5	$-2.0E-07$	$4.5E-10$	$-9.9E-13$	...
6	$-1.2E-06$	$7.7E-09$	$-2.8E-11$	$2.3E-13$
7	$-3.1E-07$	$1.4E-09$	$-1.0E-11$	$-5.0E-14$
8	$-8.8E-07$	$1.7E-08$	$-1.0E-10$	$-1.4E-13$
9	$-3.2E-07$	$-5.1E-10$	$-6.5E-12$	$6.1E-13$

which we compare several techniques applied to the Munk profile. The first two contain the execution time required at each mesh when the bisection process is repeated for each new mesh. In the second two we used a one-point Richardson extrapolation, i.e, the eigenvalue from the previous mesh was used as an initial guess and in the third row we used N-point extrapolation. In the fourth row we used N-point standard Richardson extrapolation and finally, in the fifth row we have used the modified extrapolation procedure and obtained the best results.

III. RELATION TO THE SHOOTING METHOD

Some aspects of the finite difference method that we use are closely related to the shooting method employed by previous investigators (see e.g., Refs. 3 and 4). The shooting method using the three-point difference approximation generates the value ϕ_i from two preceding values ϕ_{i-1} and ϕ_{i-2} by the formula

$$\phi_i = (\mu - a_i)\phi_{i-1} - \phi_{i-2}. \tag{19}$$

TABLE XI. Comparison of execution times using different techniques to generate initial guesses.

Number of mesh points	268	321	402	509
Bisection	3.0	3.4	4.3	5.4
1 point SRE	2.8	2.2	2.7	3.4
1 point MRE	2.8	1.5	1.9	2.4
N point SRE	3.0	2.3	2.2	2.4
N point MRE	2.9	1.6	1.7	1.6

The surface boundary condition determines the value $\phi_0 = \phi(0) = 0$. We define the value of $\phi_1 = \phi(h)$ by $\phi_1 = 1$, since the eigenfunction is known only within an arbitrary multiplicative constant. The shooting parameter μ is then determined so that $\phi_{N-1} = \phi_{N+1}$, i.e., until $\phi'(1) = 0$. Initial guesses for the value of μ must be given to apply the shooting method, e.g., the WKB method has been employed.

Initial guesses for the higher order modes may be obtained by extrapolation from the lower order modes. In addition, it follows from Sturm–Liouville theory that the jth mode has j zeros and so by counting the sign changes in the $\{\phi_i\}$ sequence it can be verified that convergence is to the desired mode.

The shooting (19) and characteristic polynomial (10) recursions are identical. Furthermore, the process of counting zeros is identified with the Sturm sequence property that the number of sign changes in the sequence is equal to the number of eigenvalues greater than μ.

An important difference between the finite difference and shooting methods is in the computation of the eigenvectors. Since one-sided shooting is unstable when integrating into intervals in which the solution decays,[13] the elements of the Sturm sequence cannot be used directly to construct the eigenvectors. Other methods, such as an analog of parallel shooting,[6] have been employed for the algebraic eigenvalue problem to partially obviate this difficulty. However, inverse iteration, which we employ in the final step of our method has the computational advantage of not being degraded as one-sided shooting or parallel shooting would be, for profiles such as multiple ducts.

[1]D. F. Gordon, "Underwater Sound Propagation-Loss Program," Naval Ocean Systems Center Rep. 393 (1979).
[2]D. C. Stickler, "Normal-Mode Program with Both the Discrete and Branch Line Contributions," J. Acoust. Soc. Am. **57**, 856–861 (1975).
[3]L. B. Dozier, "Calculation of Normal Modes in a Stratified Ocean," unpublished report.
[4]H. M. Beisner, "Numerical Calculation of Normal Modes for Underwater Sound Propagation," IBM J. Res. Dev. **18**, 53–58 (1974).
[5]W. H. Munk, "Sound Channel in an Exponentially Stratified Ocean, with Applications to SOFAR," J. Acoust. Soc. Am. **55**, 220–226 (1974).
[6]J. H. Wilkinson, *The Algebraic Eigenvalue Problem* (Clarendon, Oxford, 1965).
[7]B. N. Parlett, *The Symmetric Eigenvalue Problem* (Prentice-Hall, Englewood Cliffs, NJ, 1980).
[8]R. P. Brent, "An Algorithm with Guaranteed Convergence for Finding a Zero of a Function," Comp. J. **14**, 422–425 (1971).
[9]D. C. Joyce, "Survey of Extrapolation Processes in Numerical Analysis," SIAM Rev. **13**, 435–490 (1971).
[10]G. Dahlquist and A. Bjorck, *Numerical Methods* (Prentice-Hall, Englewood Cliffs, NJ, 1974).
[11]J. W. Paine, F. R. de Hoog, and R. S. Andersen, "On the Correction of Finite Difference Eigenvalue Approximations for Sturm–Liouville Problems," Computing **20**, 123–139 (1981).
[12]D. G. Truhlar, "Finite Difference Boundary Value Method for Solving One-Dimensional Eigenvalue Equations," J. Comp. Phys. **10**, 123–132 (1972).
[13]C. Froberg, *Introduction to Numerical Analysis* (Addison–Wesley, Reading, MA, 1965).